Synchronous Islanded Operation of an Inverter Interfaced Renewable Rich Microgrid using Synchrophasors

Synchronous Islanded Operation of an Inverter Interfaced Renewable Rich Microgrid using Synchrophasors

Lasantha Meegahapola[1], David Laverty[2*], Mats-Robin Jacobsen[2]

[1] Electrical & Biomedical Engineering, School of Engineering, RMIT University, Melbourne, VIC, 3001, Australia.

[2]School of Electronics, Electrical Engineering and Computer Science, Queens University Belfast, BT9 5AH, UK.

[*]david.laverty@qub.ac.uk

Abstract: This paper describes a novel strategy for microgrid operation and control, which enables a seamless transition from grid connected mode to islanded mode, and restoration of utility supply, without loss or disruption to loads sensitive to frequency or phase angle dynamics. A simulation study is conducted on a microgrid featuring inverter connected renewable generation, and power electronic interfaced loads. Therefore, the microgrid inherently has low inertia, which would subsequently affect the dynamic characteristics of the microgrid, in particular during mode transition. The microgrid is controlled by means of synchrophasor data to achieve synchronous island operation, enabling the microgrid to track the utility frequency and phase angle. The simulation includes synchrophasor acquisition and telecoms delays, allowing for detailed investigation of the microgrid dynamics under various mode transition scenarios, including the risk of commutation failure of the inverter sources. The proposed method is demonstrated to successfully maintain a microgrid in synchronism with the main utility grid after the transition to islanded mode without significant impact on various equipment connected to the microgrid. Thus, synchronous island operation of low inertia microgrids is feasible. This study also showed that utility supply could be seamlessly restored if the microgrid is operated as a synchronous island.

1. Introduction

Microgrids have received immense attention as one of the strategies for operating power distribution networks faced with increasing electrification and decentralisation, and infeeds from sustainable generation. A microgrid is defined as a cluster of interconnected loads and distributed generators, with a clearly defined electrical boundary and has the capability to function as an autonomous entity [1]. Microgrids will usually operate in the grid-connected mode, exchanging active and reactive power with the utility grid. However, microgrids have the option to disconnect from the main grid and operate as self-sustained autonomous islands during system contingencies [2]−[3]. In this islanded mode, the microgrid is referred to as a ‘power island’ or ‘islanded system’.

Whilst it is acceptable for power islands to operate on private premises, such as supplying a factory or commercial building with privately owned generation, it is established a practice that distributed generators must not supply utility customers with power in the absence of utility supplied generation. Such a scenario might arise if a distribution feeder suffered a fault, where a downstream distributed generator has sufficient capacity to energise the islanded loads [4]. Since distributed generators are not dispatched or controlled by the system operator, unintended islanding of utility customers puts the plant at risk from voltage and frequency excursions and raises the risk of injuries to personnel involved in the restoration of utility supply. An additional risk is the ‘out-of-synchronism’ reconnection of a power island to utility supply, which may cause destructive fault currents. For these reasons, unintentional islanding is forbidden [5]−[6].

This paper proposes the operation of a microgrid in a special mode called a 'synchronous island'. In previous work, the authors have considered an unintentional power island is forming, such that the point of common coupling (PCC) is unknown and outside the jurisdiction of the generator owner [7]. Consequently, the moment that the PCC closes and reconnects the island to the utility is not predictable, requiring the power island to be in constant synchronism with the utility supply (i.e. voltage frequency and phase-angle of the microgrid generation are controlled so that the microgrid remains in synchronism with utility supply even in the absence of a utility connection). The benefit of this technique is that instead of following the conventional anti-islanding practice and de-energizing the distributed generation [4], the microgrid remains energised throughout the loss of utility supply. Since the microgrid is always in synchronism with the utility grid, 'mode transition' from islanded mode to grid connected mode is seamless at the moment utility supply is restored at the PCC. No explicit resynchronization process is required; in effect, the microgrid is always 'resynchronizing' while in synchronous island mode. By maintaining the microgrid's synchronisation with the utility grid, transition dynamics are minimised when supply is restored, preventing disturbance to the operation of sensitive loads or generators.

Various mode-transition strategies for seamless transition are discussed in the literature [8]–[11]. The majority of these strategies are based on droop based controllers, such that the microgrid will stabilise at a new local reference frequency. Phase-angle drift at the moment of island formation will adversely affect the performance of certain loads, such as commutation failure at the variable-speed-drives (VSDs) [3]. Furthermore, since synchronous island mode necessitates control of frequency to track the utility grid phase angle, frequency droop is not possible. Instead, load sharing among the generators must be achieved using alternative methods (discussed in Section 2).

This paper is concerned with the synchronous island operation of a microgrid featuring inverter-interfaced renewable generators and power electronic interfaced loads. A simulation study has been conducted in DIgSILENT Power Factory to assess the transition dynamics of the microgrid during various mode transition scenarios. The simulation implements synchrophasor measurements to achieve the synchronous islanding controllers required for frequency and phase control and implements telecommunication delay as would be found in the practical application.

The simulation study of this paper is informed by prior work which created a physical power island featuring a large synchronous machine [7], then addressed the presence of stochastic renewable generation in a synchronous island [12]. In both cases, the presence of rotating mass in the synchronous machine provides inertia which damps microgrid dynamics. This paper contributes to this theme by addressing dynamics in a microgrid with very limited inertia, which brings new challenges and benefits. Thus, it is imperative to investigate the feasibility of islanding a renewable-rich microgrid using synchrophasor technology. The main contributions of this paper are summarised below:

- Demonstration of synchronous islanding concept on a microgrid with numerous inverter-interfaced generation sources using an enhanced phase-locked-loop (PLL) for inverter-interfaced sources.
- Phasor angle correction and grid-angle difference estimation are introduced for the phasor-angle from the PMU, which enhances the robustness of the method.
- Frequency and voltage improvement strategies are introduced for the generation sources in the microgrid during islanding, hence address the issue of commutation failure in the event of a large phase mismatch at the moment of reconnection to the main grid.

The remainder of the paper is organised as follows; Section 2 describes the concept of synchronous island operation and describes prior work in this area on synchronous machines. Microgrid simulation model is introduced in Section 3 with modelling descriptions on generation sources and loads connected to the

microgrid. The synchrophasor-based microgrid islanding and resynchronization concept are presented in Section 4. The simulation results of the synchrophasor-based microgrid islanding method are presented in Section 5. The conclusions of the study are presented in Section 6.

2. Synchronous Island Control

This section exemplifies the concept of synchronous islanding. The control challenge is explained for both single source synchronous islanding, and multiple source synchronous islanding. The use of inverter sources in the microgrid introduces further unique challenges which are discussed in Sections 4 and 5.

2.1 Concept of Synchronous Islanding

A synchronous island is a special case of a microgrid, or power island, in which the frequency and voltage phase angle of the islanded system is controlled so that it remains in synchronism with the utility grid [7]. This is typically achieved by controlling the microgrid to track the frequency and phase angle of a phasor acquired from a major substation on the interconnected utility grid. The process is similar to that of synchronising a generator for connection to the mains supply, except that the microgrid remains uncoupled to the utility grid.

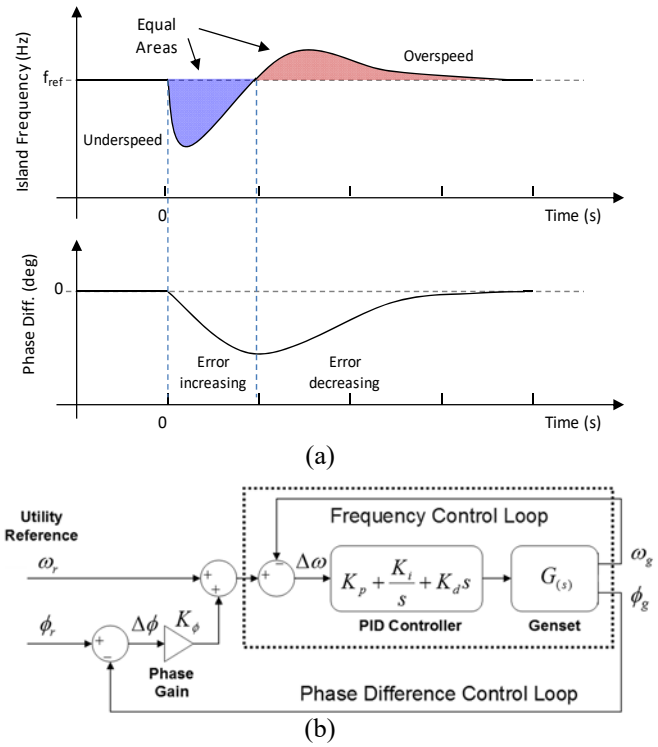

Figure 1. *(a) Frequency and phase difference when forming a synchronous Island, (b) Synchronous island control loop for a single generator.*

The concept of the synchronous island may be understood with consideration of Figure 1-(a). Consider that prior to t = 0 s, the microgrid has been operating at the same frequency as the utility grid, with a phase angle difference of 0°. At time t = 0 s the load demand on the island has increased, leading to a negative frequency excursion. This has the effect of causing the phase angle of the island with respect to the utility grid to diverge. In a traditional power island, the generator governor would act to restore nominal frequency without considering the phase angle difference. In a synchronous island, the generator is controlled such that it temporarily over-speeds until the phase angle difference is returned to 0°.

Considering that phase is the integral of frequency error about nominal frequency, then an equal area criterion exists.

The authors have previously developed controllers for operating a microgrid comprised of synchronous generators in the synchronous islanded mode [12]. In Figure 1-(b), a primary control loop adjusts the frequency of the islanded generator, ω_g, to match the frequency of the utility reference, ω_r. A classical PID controller is employed, with integral action ensuring that the frequency error ($\Delta\omega$) tends to zero. A secondary control loop is responsible for phase control and operates by biasing the frequency error by a proportion of the phase error ($K_\phi\Delta\phi$). The integral term within the frequency loop acts to reduce the phase error to zero.

2.2 Multiple Generator Synchronous Island

In a conventional power system, generation is usually dispatched by means of frequency droop (see Figure 2-(a)). Since in a synchronous island the frequency of the islanded system is not a function of generation and demand, but depends instead on the reference signal from the utility grid, a conventional frequency droop dispatch is not possible. This poses a problem to the operation of a synchronous island with more than one generator.

A rudimentary approach would be to allow generators to pick up and shed load as they respond to changes in frequency set-point. However, different generator types will have different dynamics. Some units will pick up / shed load faster than others. As such this mechanism alone will be unlikely to yield an optimal or preferred generation dispatch. Furthermore, it is possible that the dynamics between two or more generators will set-up oscillating behaviour which will destabilise the synchronous island.

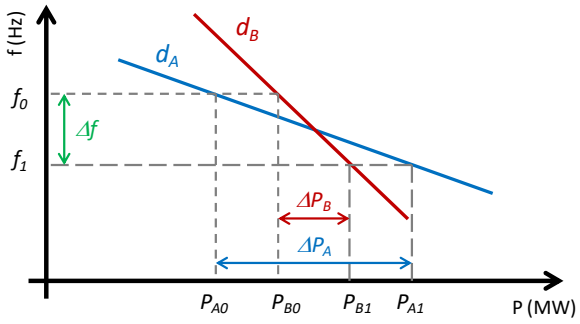

(a)

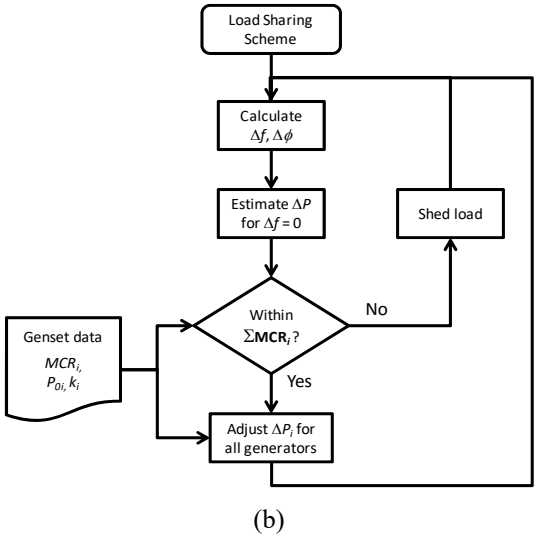

(b)

***Figure 2**. (a). An example of droop load-frequency control to provide load sharing between two or more machines. (b) Flow diagram of load sharing scheme for synchronous islands.*

A communication-based centralised load dispatch method is employed in [14], and this mechanism (see Figure 2-(b)) uses information which characterises the generators within the island. This includes, for each generator '*i*', its maximum continuous rating (MCR_i), nominal power output set-point (P_{0i}), and load pick-up gain (k_i). The latter is conceptually equivalent to droop in the synchronous island.

The load sharing scheme acts as a supervisory control loop, updating the power output set-point of each generator within the synchronous island at time intervals of seconds. By design, this is a much slower update rate than the phase/frequency control loops which operate autonomously at each generator. Thus load sharing is a secondary response. The gain of the phase/frequency control loops are set such that certain machines are preferred to control the island frequency, discouraging machines oscillating against each other. In the event that the power demand of the microgrid exceeds available generation (ΣMCR_i) then load shedding may be employed. Load shedding is necessary for the event that there is insufficient supply whether the island operates in synchronous mode or as a traditional power island.

2.3 Configuration, Reference Source and Performance

A single machine synchronous island control system requires a phasor measurement unit (PMU) at the reference location, a PMU at the generator and a telecoms channel to deliver the reference synchrophasor to the controller local to the generator. Although the capital costs may appear prohibitive, the authors demonstrate that the PMU can be constructed using commodity low-cost development boards [13]. The control algorithms can also operate on low-cost computing hardware, such as on a Raspberry Pi as described in [14]. As for operational costs, the bandwidth and latency requirements are not arduous. Synchrophasors require circa 75 kbps throughput, and the authors have shown that the control system will operate with latencies as high as 300 ms [7]. In [15] the authors show that standard enterprise or domestic telecoms delivery technologies are sufficient to achieve this, meaning that no special arrangements are needed for the synchronous islanding scheme where broadband internet is already present.

A reference source should be chosen that is regarded to be electrically secure; that is to say, that it should not itself be vulnerable to islanding. A major transmission substation would be preferred. Multiple reference locations may also be used, and a filter applied to reject anomalous data. The authors intend to consider this in future work. Disturbances in the main utility grid would lead to the synchronous island attempting to follow suit. Since this would be undesirable, power quality metrics or synchrophasor quality metrics such as Goodness-of-Fit [16] could be used to reject momentary disturbances. Long-term disruption to the reference source would necessitate the synchronous island transition to normal islanded mode.

In previous work concerned with synchronous island operation of a diesel generator set, the authors considered keeping phase deviation in the range ±60° as a performance target. This is related to the electromechanical limits of a synchronous machine [13]. The authors demonstrated that on a 50 kVA machine, load acceptances of up to 25% maximum continuous rating were possible whilst maintaining the performance target. In this work, it is necessary to consider the attributes of inverter sources. Whilst [3] indicates thresholds of ±20° is necessary to avoid commutation failure, the low inertia of an inverter based microgrid is advantageous to achieving this performance target.

3. The Microgrid Simulation Model

A commercial building microgrid simulation model was developed in DIgSILENT Power Factory by considering characteristics of various types of loads and generation connected to an actual commercial building microgrid [1], [18]. A schematic of the microgrid simulation model is shown in Figure 3.

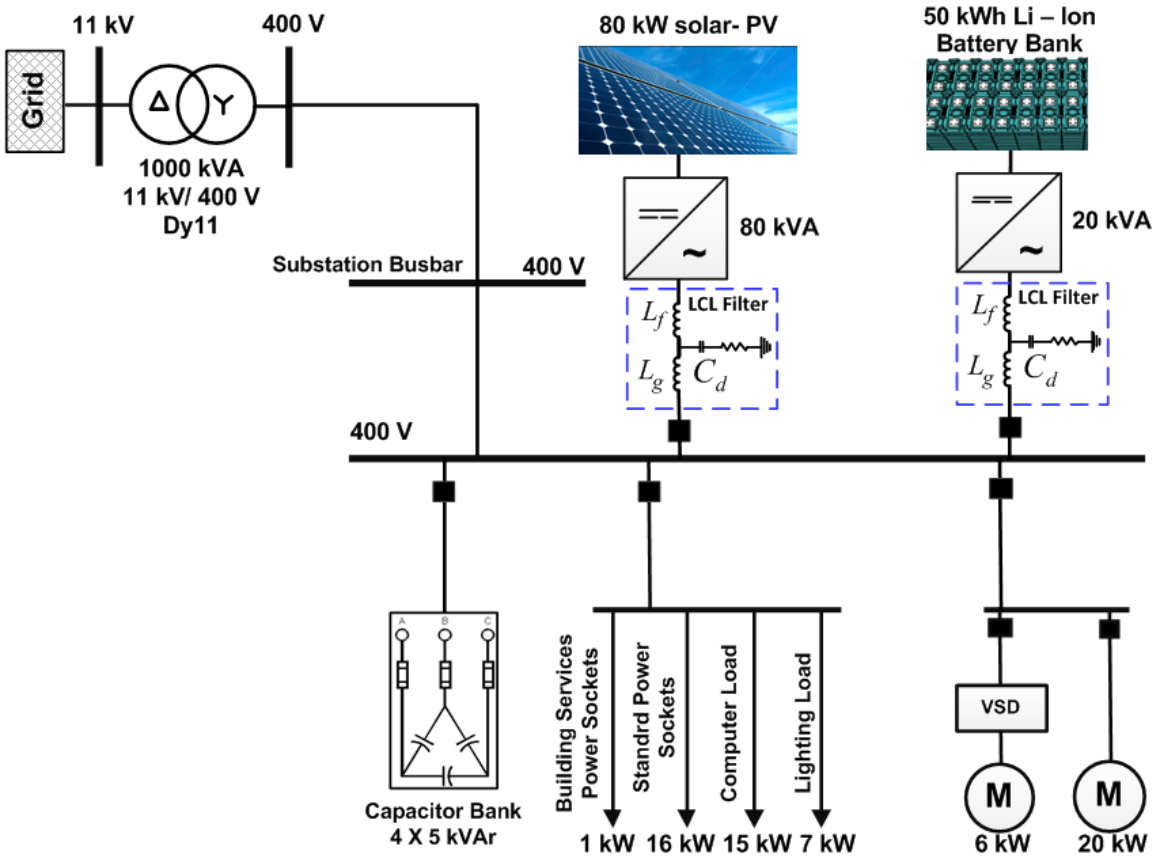

Figure 3. *The microgrid simulation model.*

The microgrid simulation model comprises an 80 kW solar-PV generation system equipped with an 88 kVA inverter and a 50 kWh Li-Ion battery bank with a 22 kVA inverter. In addition, a 30 kVAr switched capacitor bank provides the steady-state reactive power requirement for the microgrid based on the voltage at the main 400 V busbar in the microgrid.

3.1 Solar-PV Model

The dynamic simulation model of the solar-PV system consists of the following components: the solar-PV array, three-phase voltage source inverter (VSI), DC-DC converter with the maximum power-point tracking (MPPT) system, and an LCL filter. The 80 kW solar-PV array is modelled with an appropriate number of series and parallel solar-PV modules. The design parameters of the solar-PV array are shown in Table 1 (see Appendix). The solar-PV array model is capable of responding to varying solar irradiation and ambient temperature conditions. The solar-PV module characteristics are based on a commercially available actual solar module [19]. The MPPT system is designed based on the incremental conductance algorithm [20].

The LCL filter parameters (L_g, C_d, L_f) are selected based on the method outlined in [20]. The DC link capacitor, input filter capacitor and DC coupling inductor sizes were determined based on [22]. An average converter model is used for representing the three-phase VSI, and it controls both voltage and frequency of the microgrid using droop controllers. The frequency droop activates when the microgrid main busbar frequency deviates from ±0.5 Hz, while the voltage droop activates when microgrid main busbar voltage deviates from ±2 V.

3.2 Battery Energy Storage System

The 50 kWh battery energy storage system is comprised of 68 series connected cells. Each cell has a capacity of 50 Ah with a maximum full charge voltage of 14.6 V, and values are based on specifications

given in [23]. The charging characteristics are incorporated into the battery model while the active and the reactive power control capabilities are integrated into the converter model.

The charge controller determines the state-of-charge (SOC) of the Li-Ion battery bank, and based on the requirements dictated by the microgrid energy management system; the charge controller will either charge or discharge the battery system [18]. In addition, it will maintain the DC link at a constant voltage by controlling the duty cycle (α) of the DC-DC boost converter. The battery energy storage can also control both voltage and frequency of the microgrid. The parameters associated with the LCL filter (L_g, C_d, L_f), DC link capacitor and input filter are determined based on the same method used for the PV system.

It must be noted that the battery energy storage system can control the microgrid voltage and frequency continuously. Hence, voltage and frequency of the microgrid main busbar are continuously monitored, and subsequently, voltage and frequency errors are determined while comparing with the respective reference values. Then, voltage and frequency errors are feed through PI controllers to update the active and reactive power references of the battery energy storage system.

3.3 Modelling of Loads

Different load types are connected to the microgrid model representing various loads connected to the commercial building microgrid. In particular, various motor loads (e.g. VSD and direct on-line (DOL) motor loads) are represented in the microgrid model as aggregated motor loads, which are essential to characterise the dynamics accurately during mode transition. The VSD was modelled with a front-end diode rectifier and an inverter system, while the load dynamics are represented by respective load characteristics (e.g. pump).

The front-end controlled rectifier will maintain the DC link voltage constant by varying the thyristor firing angle based on the AC voltage at the Main Distribution Board. Also, the VSD controller has the capability for soft-start, and the drive speed can also be set constant by changing the speed reference. The direct-on-line (DOL) induction motor load is the most dominant load component in the microgrid (20 kW), which represents heat pumps in the microgrid. The DOL motor loads were modelled with an induction motor model and incorporate the respective load characteristics (i.e. fan and pump models) in order to replicate the actual load behaviour. In addition, a soft-starter is also modelled at the front end of the induction motor.

The complex load model given in DIgSILENT Power Factory has been employed to represent the other loads (e.g. lighting, computer and other office loads) in the microgrid. Further information on modelling of a commercial building microgrid is explained in [3], [18].

4. Synchronous Island Control and Resynchronization of Microgrid

The inverter-interfaced renewable sources are typically phase-locked to the local busbar, which is in synchronism with the main grid during the grid-connected mode. Therefore, the principle challenge here is to maintain synchronism with the main grid when the microgrid is islanded. The proposed synchrophasor-based islanding strategy relies on the synchrophasor obtained from a PMU installed at a different location in the network. This proposed strategy will enable the microgrid to maintain synchronism with the main grid when the microgrid becomes islanded from the distribution network. Figure 4 illustrates the concept of synchrophasor-based islanding strategy for the microgrid.

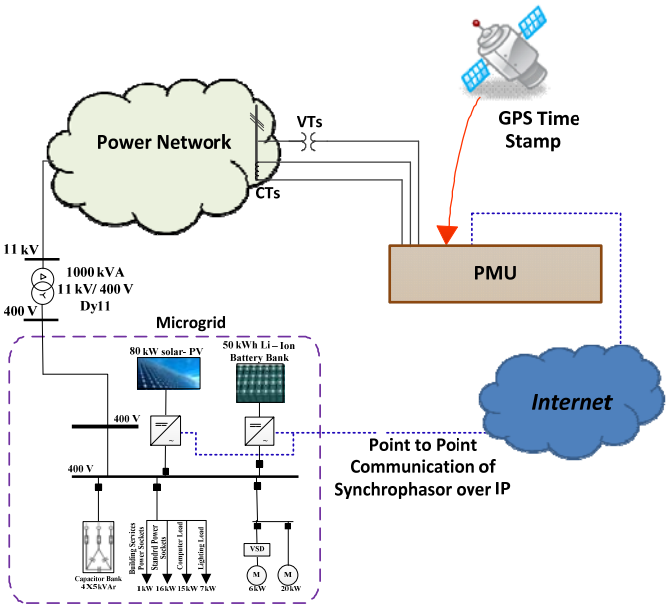

(a)

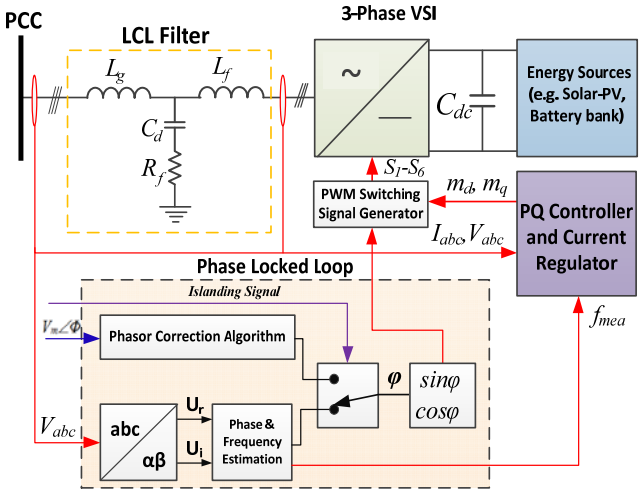

(b)

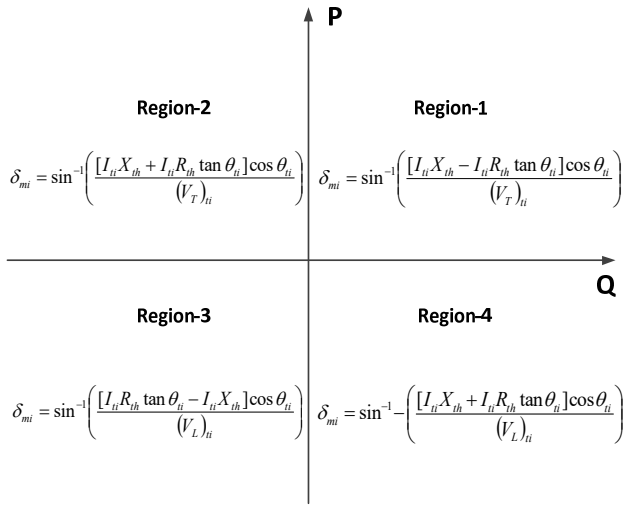

(c)

Figure 4. *(a) Synchrophasor based microgrid islanding strategy, (b). Proposed synchronising approach for inverter-interfaced renewables, (c) δ_{mi} angle estimation.*

Illustrated in Figure 4-(a), a PMU installed at a different location (e.g. grid substation) in the network sends a synchrophasor to the microgrid, and then it will be deployed by the inverter-interfaced renewable sources when the microgrid is islanded. This will enable microgrid inverters to be phase-locked to the main grid. The proposed control architecture for inverter-interfaced renewable sources is shown in Figure 4-(b).

Shown in Figure 4-(b), prior to islanding, the PLL is operating based on the local reference. However, once an islanding event is detected, it will switch to the synchrophasor obtained from a PMU located at another location on the network. Once the reference phasor is obtained from the synchrophasor, following phasor correction algorithm is applied to determine the final phasor:

$$\varphi(t_i) = \delta_{mi} + \Phi(t_i) \quad (1)$$

Where, $\Phi(t_i)$, and δ_{mi} denote phase angle measured at time t_i, and the angle difference between the microgrid point of common coupling (PCC), and the PMU installed location at time t_i respectively. The δ_{mi} is determined based on the operating quadrant of the microgrid (power exchange at the PCC – see Figure 4-(c)). For example, if the microgrid exports both active and reactive power prior islanding (Region-1 in Figure 4-(c)), then δ_{mi} is given as; $\delta_{mi} = \sin^{-1}\left(I_{ti}X_{th} - I_{ti}R_{th}\tan\theta_{ti}\right]\cos\theta_{ti}/\left(V_T\right)_{ti}\right)$.

The δ_{mi} is calculated based on the vector diagram drawn between the voltage vector at microgrid PCC (V_T), and the voltage vector at the PMU location (V_L). I, θ, X_{th} and R_{th} denote magnitude of the current flow from/to microgrid if the microgrid is connected to the grid, power factor angle at microgrid PCC, the Thevenin's equivalent reactance and resistance between the microgrid PCC and PMU location respectively. It must be noted that δ_{mi} is updated at each time t_i. The corrected phase $\varphi(t_i)$, can be further modified by employing the phase correction algorithm in [7] to address the communication latencies and packet loss, and hence it would improve the stability of the microgrid.

5. Islanding and Resynchronization Performance Evaluation using Synchrophasor

The proposed synchrophasor-based islanding and resynchronization concept is examined under various operating conditions for the microgrid (i.e. power import and power export) and various synchrophasor communication latencies. In this simulation, it is assumed that the synchrophasor is obtained from a PMU installed at an upstream location of the 11 kV feeder. The generation and the load demands for power import and export scenarios are given in Table 1.

Table 1 Generation Portfolio of the Microgrid during Islanding

Scenario	Solar-PV	Battery (initial SOC-80%)	Total Load
Export mode	74 kW	8 kW Charging	57.5 kW
Import mode	50 kW	8 kW Discharging	65 kW

The battery system's initial SOC is 80%.

5.1 Islanding using Synchrophasors during Power Import

Figure 5 illustrates a comparison of microgrid performance between the proposed synchrophasor-based islanding technique and conventional local reference based technique during power import mode.

The microgrid has experienced a voltage dip of 0.02 pu when the phase locked to the synchrophasor during the transition to islanding mode. However, it indicates substantial improvement in the phase-angle drop. For example, phase angle drop has improved by 3° when islanding with synchrophasor. Microgrid frequency has also improved by 0.03 Hz when synchrophasor are used for islanding. Therefore,

synchrophasor could be used as a successful method for islanding without any adverse impact on mode transition.

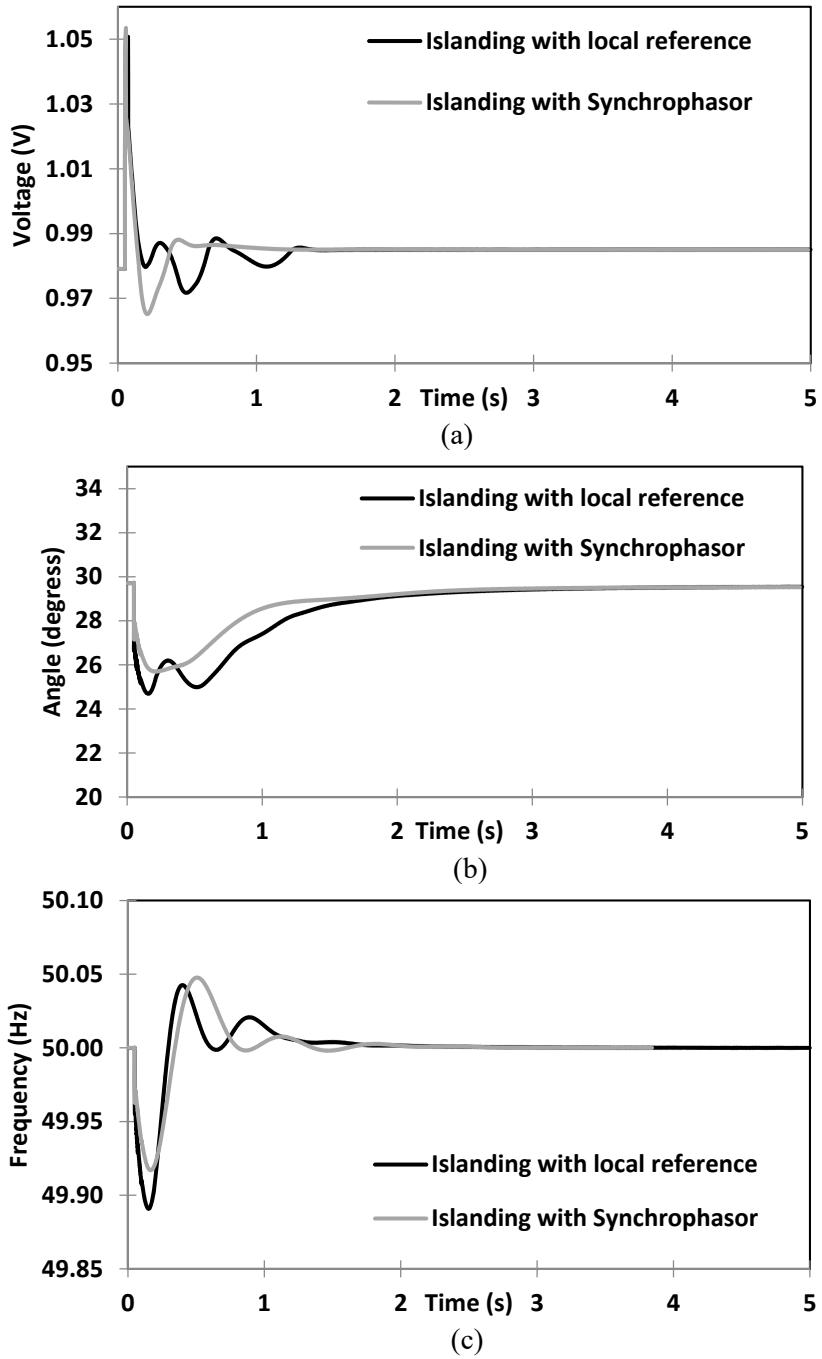

Figure 5. *Comparison of islanding with and without synchrophasor during power import mode; (a) Voltage magnitude, (b) Voltage angle, (c) Microgrid frequency.*

Figure 6 illustrates the microgrid performance comparison between the proposed synchrophasor islanding technique and conventional local reference technique during power export mode.

According to Figure 6, the instantaneous phase-angle shift has substantially decreased (e.g. by 4°) when synchrophasor are employed for islanding. Furthermore, initial frequency transient has also decreased by 0.02 Hz despite increased oscillations in the frequency. Power export mode also proved that microgrid

could be islanded without significant impact on microgrid operation. Therefore, the VSD motor loads remained connected during the transition to islanded mode.

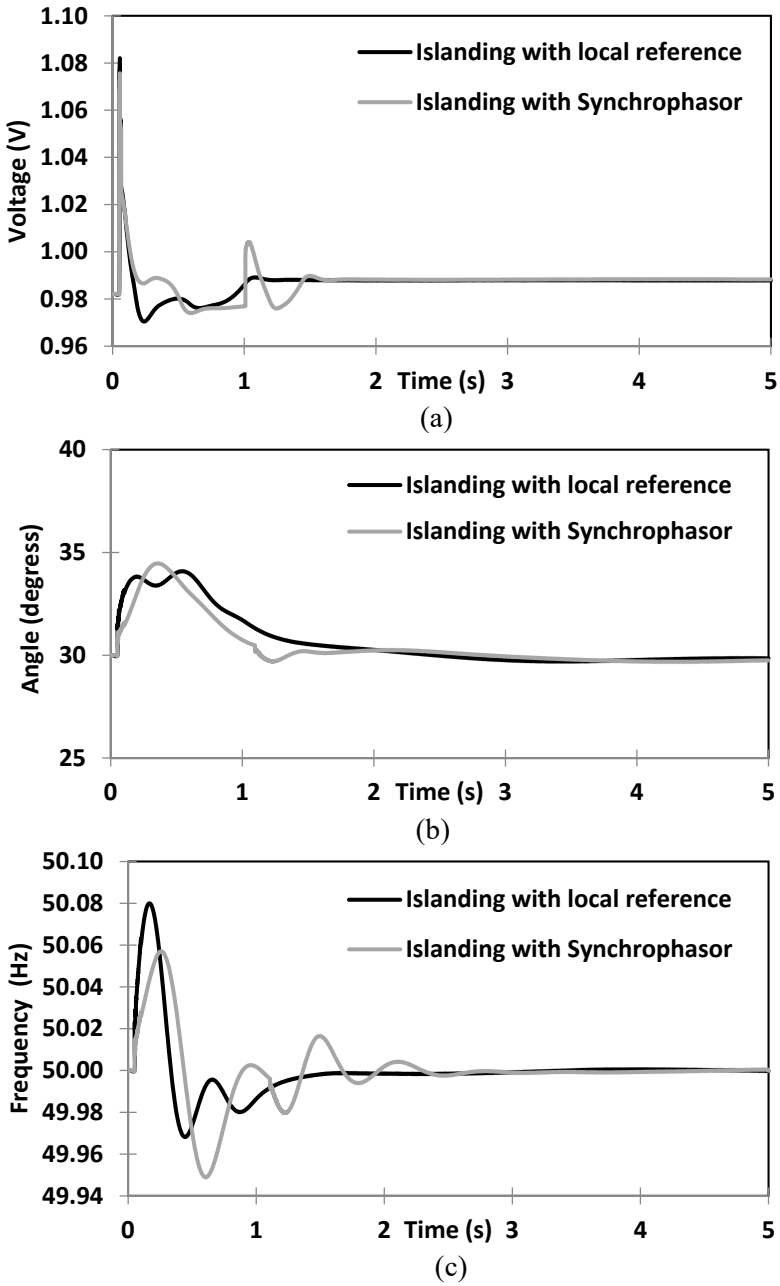

Figure 6. *Comparison of islanding with and without synchrophasor during power export mode; (a) Voltage magnitude, (b) Voltage angle, (c) Microgrid frequency.*

5.2 Resynchronization with Grid

Further simulations are carried out to investigate the voltage transients when resynchronizing the islanded microgrid with the main grid. Figure 7 illustrates the three-phase voltage waveforms when the islanded microgrid resynchronizes with the main grid. The microgrid is reconnected at t = 2 s. Note that when the microgrid is reconnected as it operates under local reference, a resynchronization algorithm was not employed in order to benchmark with the proposed technique.

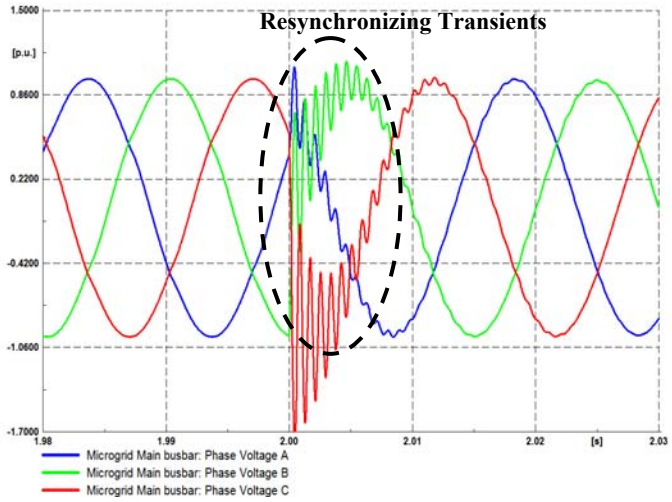

(a)

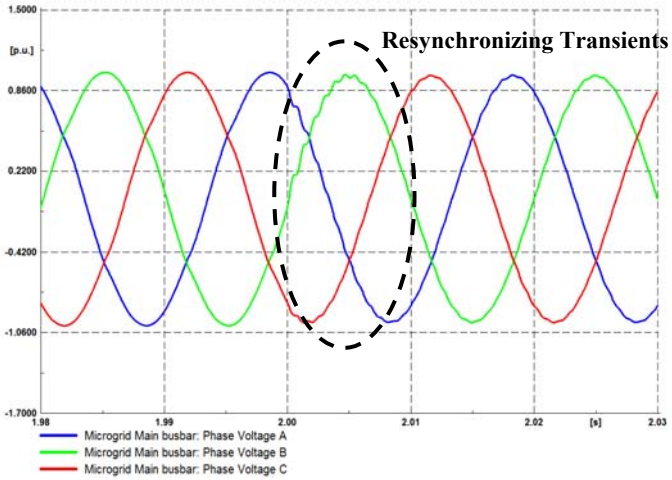

(b)

Figure 7. *Re-synchronisation of the microgrid; (a) islanded operation with a local reference, (b) islanded operation with synchrophasor.*

Shown in Figure 7-(a), significant large voltage transients could be seen in the voltage waveforms when the microgrid is reconnected to the grid when operating with a local reference; this could be detrimental to loads and inverter-interfaced sources in the microgrid. However, with synchrophasor-based islanding strategy, mode transition to grid connected mode is seamless, and significantly less distortion and phase angle shift can be seen in the voltage waveforms.

5.3 Impact of Communication Latencies

The communication latency is one of the issues with the synchrophasor-based islanding method. As mentioned in [6], communication latencies could potentially lead to instability. Therefore, the transition to islanded mode is investigated with different communication latencies associated with the synchrophasor, and microgrid dynamics are shown in Figure 8. It must be noted that microgrid is operating under power import mode, and the power deficit is managed by the battery energy storage system.

When the communication latency increases, the microgrid experiences larger voltage and frequency variations during synchronous islanding. However, the microgrid has recovered to nominal operating

conditions within 1.5 s. According to Figure 8-(d), even with 200 ms communication latency the microgrid could be reconnected to the main grid without significant voltage transients or phase shift.

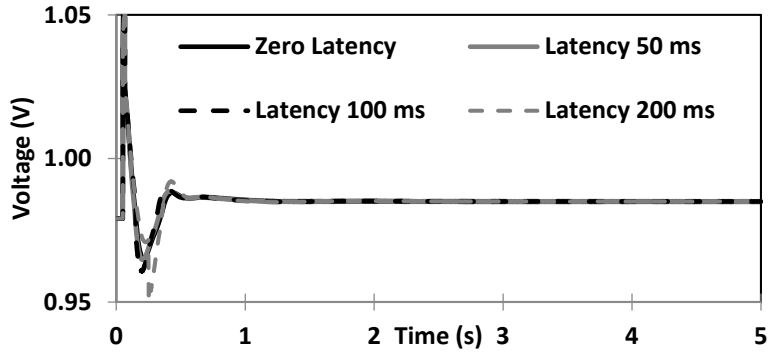

(a)

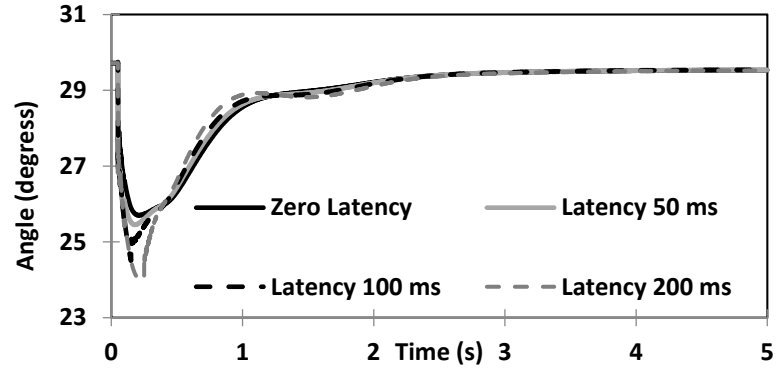

(b)

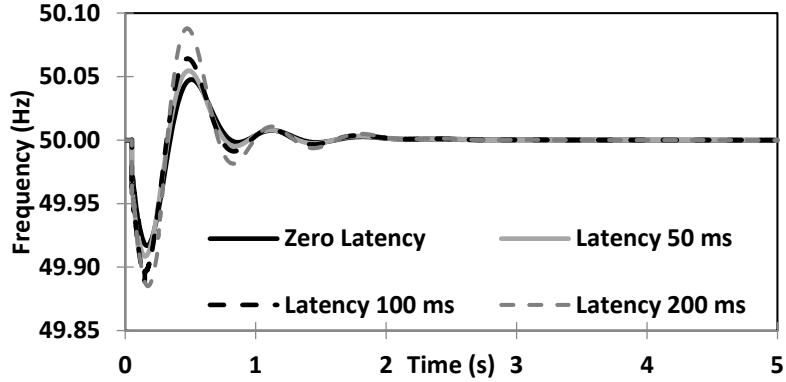

(c)

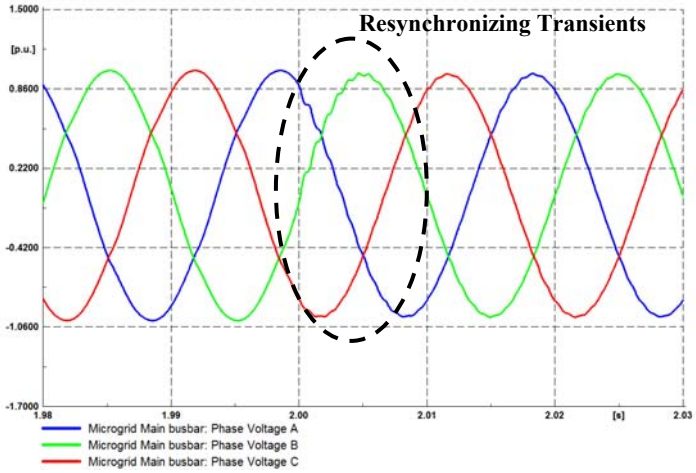

(d)

Figure 8. *Synchrophasor based islanding with different communication latencies; (a) Voltage magnitude, (b) Voltage angle, (c) Microgrid frequency, (d) Re-synchronisation of the microgrid with a 200 ms communication latency for the synchrophasor.*

5.4 Synchronous Islanding Performance with Synchronous and Inverter Interfaced Sources in Microgrid

An additional scenario was simulated in this section with a 20 kW synchronous generator added to the microgrid. For the synchronous generator, Woodward Diesel Governor [24] and IEEEX1 automatic voltage regulator (AVR) [25] models have been adopted. Power import mode was considered in this scenario, and solar-PV system power output has been decreased to 30 kW since the diesel generator provides 20 kW to the microgrid. Also it must be noted that the synchrophasor signal is only used at the inverter interfaced sources (i.e. Solar-PV and Battery energy storage system), thus the diesel generator is synchronized with the frequency at the microgrid 400 V busbar. Figure 9 illustrates a comparison of microgrid performance between the proposed synchrophasor-based islanding technique and conventional local reference based technique.

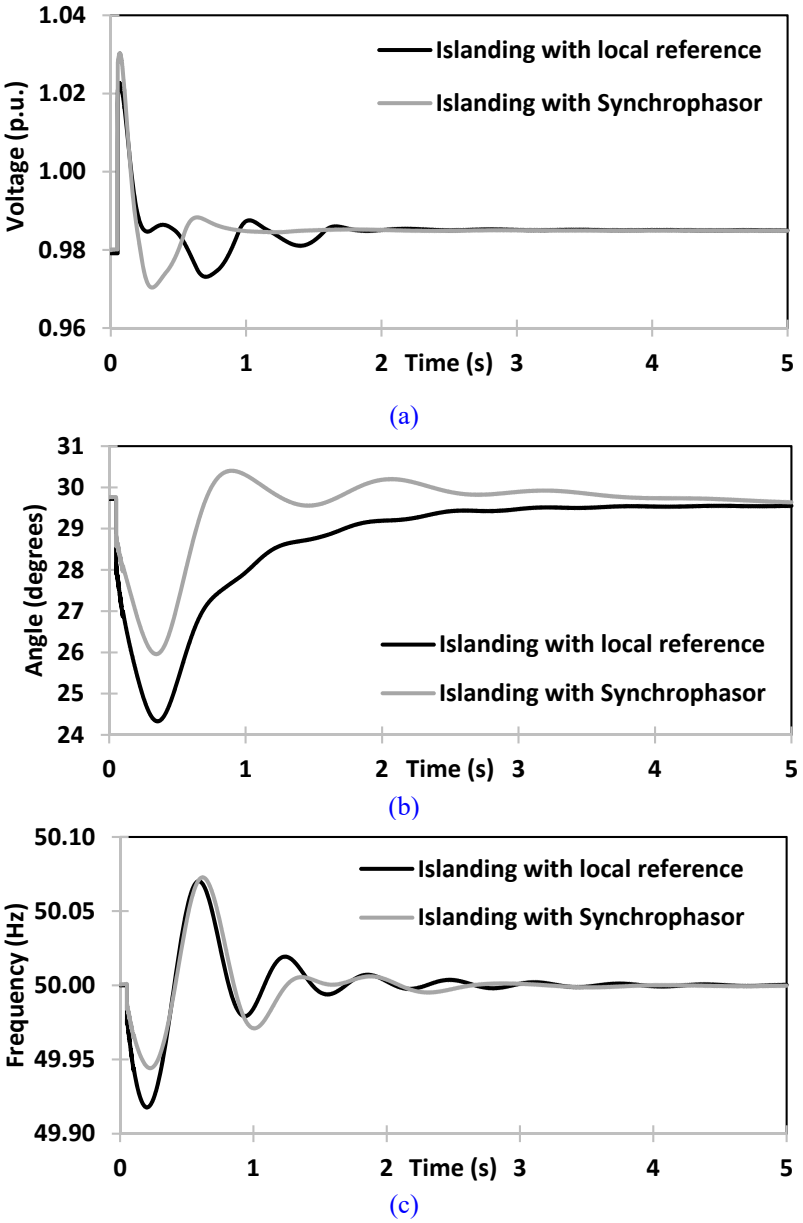

Figure 9. *Comparison of islanding with and without synchrophasor during power import mode for a Microgrid with Synchronous & Inverter interfaced Generation Sources; (a) Voltage magnitude, (b) Voltage angle, (c) Microgrid frequency.*

According to Figure 9, a much lesser frequency drop could be observed in this microgrid, in comparison to the microgrid with inverter interfaced sources (see Figure 5) during islanding condition. For example, frequency has decreased by 0.05 Hz during islanding for the synchronous islanding scenario in the microgrid with both synchronous and inverter interfaced generation sources while for the microgrid with the inverter interfaced sources frequency has decreased by 0.08 Hz during islanding. This improvement is mainly due to the improved inertia in the microgrid, due to the stored kinetic energy in the synchronous generator. In addition, much better performance could also be observed in voltage angle in this microgrid in comparison to the microgrid with only inverter interfaced sources. Therefore, this scenario illustrates the fact that once the proposed synchronous islanding scheme is implemented on inverter interfaced sources, then conventional synchronous generators can track the frequency/angle without additional control modifications on the generator governor.

6. Conclusions

This paper has illustrated the viability of operating a microgrid comprised of inverter-interfaced generation sources as a synchronous island. Operating in this mode yields the benefit that the microgrid may be reconnected to the main utility grid at any moment in time without the need to follow a resynchronization procedure. This is essential when the PCC is outside of the generator owner's control, as may be the case when a power island is formed unintentionally. Since faults in distribution networks are more common than high voltage network faults, this strategy will enable improvements to the reliability of the distribution grid by operating healthy sections of the distribution grid as synchronous islands whilst disconnected from the main grid.

It is shown that under various operating conditions, and with varying communication latencies, that the microgrid can maintain synchronism with the main grid. The control strategy employed by the authors minimises phase shift and frequency variation. Consequently, voltage transients are reduced at the moment of reconnection, preventing commutation failure of the inverter sources. Further research should be conducted to minimise the voltage dip during the transition to synchrophasor islanding.

Practical implementation of the proposed scheme will be possible provided adequate consideration is paid to the issues identified, namely minimising phase shift at the moment of island formation, load sharing between generators, and design of telecoms latency to suit control requirements.

With regards the choice of location for the reference synchrophasor, consideration must be given to the possibility that the reference location could itself suffer an outage, or that a transient event may affect that reference location which would be undesirable to replicate in the microgrid during synchronous island operation. The use of multiple reference locations will mitigate concern regards an outage. Use of quality indicators, such as Goodness of Fit for synchrophasor [16], provides a means of informing the synchronous island controller to reject irregular data. Further work in this area will reveal appropriate thresholds for such quality metrics. This study has shown very promising simulation results, however further studies are required to improve the fidelity of the proposed technique.

References

[1] 'Summary Report: 2012 DOE Microgrid Workshop', http://energy.gov/sites/prod/files/2012%20Microgrid%20Workshop%20Report%2009102012.pdf, accessed 2017.

[2] Tan, Y., Meegahapola, L., Muttaqi, K.: 'A Review of Technical Challenges in Planning and Operation of Remote Area Power Supply Systems', Renewable & Sustainable Energy Reviews, 2014, 38, pp 876-889. **DOI: 10.1016/j.rser.2014.07.034**

[3] Meegahapola, L., Robinson, D., Agalgaonkar, A., Perera, S., Ciufo, P.: 'Microgrids of Commercial Buildings: Strategies to Manage Mode Transfer from Grid-Connected to Islanded Mode', IEEE Trans. Sust. Energy, 2014, 5, (4), pp 1337-1347. **DOI: 10.1109/TSTE.2014.2305657**

[4] Laverty, D.M., Best, R.J., Morrow, D.J.: 'Loss-of-mains protection system by application of phasor measurement unit technology with experimentally assessed threshold settings,' IET Generation, Transmission & Distribution, 2015, 9, (2), pp 146-153. **DOI: 10.1049/iet-gtd.2014.0106**

[5] 'Engineering Recommendation G59/3 - Recommendations for the Connection of Generating Plant to the Distribution Systems of Licensed Distribution Network Operators', ENA, Sep. 2013.

[6] IEEE Std 1547.4-2011: 'IEEE Guide for Design, Operation, and Integration of Distributed Resource Island Systems with Electric Power Systems', 2011. **DOI: 10.1109/IEEESTD.2011.5960751**

[7] Best, R.J., Morrow, D.J., Laverty, D.M., Crossley, P.A.: 'Synchrophasor Broadcast over Internet Protocol for Distributed Generator Synchronization', IEEE Trans. Power Deliv, 2010. 25, (4), pp 2835-2841. **DOI: 10.1109/TPWRD.2010.2044666**

[8] Vandoorn, T.L., Meersman, B., De Kooning, J.D.M., Vandevelde, L.: 'Transition from Islanded to Grid-Connected Mode of Microgrids With Voltage-Based Droop Control', 2013. IEEE Trans. Power Syst., 28, (3), pp 2545-2553. **DOI: 10.1109/TPWRS.2012.2226481**

[9] Bloemink, J.M., Iravani, M.R.: 'Control of a Multiple Source Microgrid With Built-in Islanding Detection and Current Limiting', IEEE Trans. Power Deli., 2012, 27, (4), pp 2122-2132. **DOI: 10.1109/TPWRD.2012.2198497**

[10] Mohamed, Y.A.R.I., Radwan, A.A.: 'Hierarchical Control System for Robust Microgrid Operation and Seamless Mode Transfer in Active Distribution Systems', 2011, IEEE Trans. Smart Grid, 2, (2), pp 352-362. **DOI: 10.1109/TSG.2011.2136362**

[11] Wang, J., Chang, N.C.P., Feng X., Monti, A.: 'Design of a Generalised Control Algorithm for Parallel Inverters for Smooth Microgrid Transition Operation', 2015, IEEE Trans. Industry. Electr., 62, (8), pp 4900-4914. **DOI: 10.1109/TIE.2015.2404317**

[12] Best, R.J., Morrow, D.J., Laverty, D.M., Crossley, P.A.: 'Techniques for multiple-set synchronous islanding control', IEEE Trans. Smart Grid, 2011, 2, (1), pp 60-67. **DOI: 10.1109/TSG.2010.2100833**

[13] Zhao, X., Laverty, D.M., McKernan, A., Morrow, D.J., McLaughlin, K., Sezer, S.: 'GPS Disciplined Analogue to Digital Converter for Phasor Measurement Applications', IEEE Trans. on Instrumentation and Measurement, 2017, 66, (9), pp 2349 – 2357. **DOI: 10.1109/TIM.2017.2700158**

[14] Jacobsen, M.R., Laverty D., Best, R.J.: 'A laboratory experiment of single machine synchronous islanding using PMUs and Raspberry Pi — A platform for multi-machine islanding', Proc. 2016 IEEE Power and Energy Society General Meeting (PESGM), Boston, MA, 2016, pp. 1-4. **DOI: 10.1109/PESGM.2016.7741761**

[15] Laverty, D.M., Kang, L.I., Morrow. D.J.: 'Secure data networks for electrical distribution applications', Journal of Modern Power Systems and Clean Energy, 2015, 3, (3), pp 447-455. **DOI: 10.1007/s40565-015-0121-3**

[16] Riepnieks A., Kirkham, H.: 'An Introduction to Goodness of Fit for PMU Parameter Estimation', IEEE Trans. on Power Delivery, 2017, 32, (5), pp 2238 – 2245. **DOI: 10.1109/TPWRD.2016.2616761**

[17] Best, R.J., Morrow, D.J., Crossley, P.A.: 'Current transients in the small salient-pole alternator caused by sudden short-circuit and synchronisation events', IET Electric Power Applications, 2010, 4, (9), pp 687-700. **DOI: 10.1049/iet-epa.2009.0263**

[18] Meegahapola, L., Robinson, D.: 'Chapter 7: Dynamic Modelling, Simulation and Control of a Commercial Building Microgrid', in Jayaweera, D. (Ed.): 'Smart Power Systems and Renewable Energy Systems Integration' (Springer International Publishing, Cham, Switzerland, 2016), pp. 119-140. **DOI: 10.1007/978-3-319-30427-4_7**

[19] 'REC Peak energy series', http://www.recgroup.com, accessed Apr. 2017.
[20] Hussein K.H., Mota, I.: 'Maximum photovoltaic power tracking: An algorithm for rapidly changing atmospheric conditions', IEE Proceedings Generation Transmiss. Distrib., 1995, 142, (1), pp 59–64. **DOI: 10.1049/ip-gtd:19951577**
[21] Liserre, M., Blaabjerg F., Hansen S.: 'Design and Control of an LCL-Filter-Based Three-Phase Active Rectifier', IEEE Trans. Industry Applications, 2005, 41, (5), pp 1281-1291. **DOI: 10.1109/TIA.2005.853373**
[22] Feng, G., Ding, L., Loh, P.C., Tang, Y., Wang, P.: 'Indirect dc-link voltage control of two-stage single-phase PV inverter', IEEE Energy Conversion Congress and Exposition (ECCE 2009), Sept. 2009. **DOI: 10.1109/ECCE.2009.5316399**
[23] 'Smart Battery:12V 50AH Lithium Ion Battery Data Sheet', http://www.lithiumion-batteries.com, accessed Apr. 2017.
[24] IEEE Power & Energy Society, 'Dynamic Models for Turbine-Governors in Power System Studies', (IEEE PES, 2013).
[25] IEEE Std 421.1-2007: 'IEEE Standard Definitions for Excitation Systems for Synchronous Machine', 2007. **DOI: 10.1109/IEEESTD.2007.385319**

Appendix-A

Table A.1. Solar-PV Array Parameters

Parameter	Value
Open-circuit Voltage (STC) of Module	43.8 V
MPP Voltage (STC) of Module	35 V
Short-circuit Current (STC) of Module	5 A
MPP Current (STC) of Module	4.58 A
Series Modules	20
Parallel Modules	25